



# The effect of NaCl on the rheological properties of suspension containing spray dried starch nanoparticles

Ai-min Shi<sup>a,1</sup>, Dong Li<sup>a,1</sup>, Li-jun Wang<sup>b,\*</sup>, Benu Adhikari<sup>c</sup>

<sup>a</sup> College of Engineering, China Agricultural University, P.O. Box 50, 17 Qinghua Donglu, Beijing 100083, China

<sup>b</sup> College of Food Science and Nutritional Engineering, China Agricultural University, Beijing, China

<sup>c</sup> School of Health Sciences, University of Ballarat, VIC 3353, Australia

## ARTICLE INFO

### Article history:

Received 15 May 2012

Received in revised form 30 June 2012

Accepted 7 July 2012

Available online 16 July 2012

### Keywords:

Rheological properties

Starch nanoparticles

Spray drying

NaCl

Suspension

## ABSTRACT

The effect of NaCl on the rheological properties of suspensions containing spray dried starch nanoparticles produced through high pressure homogenization and emulsion cross-linking technique was studied. Rheological properties such as continuous shear viscosity, viscoelasticity and creep-recovery were measured. NaCl (5–20%, w/w) was found to lower viscosity quite significantly ( $p < 0.05$ ), enhance the heat stability and weaken their gelling behavior compared to starch-only suspension. NaCl reduced both the storage and loss moduli of suspension within the frequency range (0.1–10 rad/s) studied. However, NaCl brought higher speed of reduction on the storage modulus than on the loss modulus, which resulted into large increase in loss angle. The creep-recovery behavior of suspension was affected by NaCl and the recovery rate was highest (86%) at 15% NaCl. The Cross, the Power law and the Burger's models followed the experimental viscosity, storage and loss moduli, and creep-recovery data well with  $R^2 > 0.97$ .

© 2012 Elsevier Ltd. All rights reserved.

## 1. Introduction

Starch and its derivatives are commonly used in food, pharmaceutical, textile and chemical industries (BeMiller & Whistler, 2009; Granö, Yli-Kauhaluoma, Suortti, Käkä, & Nurmi, 2000; Le Corre, Bras, & Dufresne, 2010; Singh, Dartois, & Kaur, 2010; Singh, Singh, Pandey, & Sanghi, 2010). Starch nanoparticle is a novel product derived from starch and it can be produced through crosslinking reaction between the starch and cross-linker (such as sodium trimetaphosphate and phosphorus oxychloride). These starch nanoparticles have drawn considerable research interest due to their potential and usefulness in high value pharmaceutical and medical industries (Le Corre et al., 2010; Simi & Emilia Abraham, 2007). There are many publications reporting the preparation, drying, structure analysis and functional performance of starch nanoparticles (Chin, Pang, & Tay, 2011; Li, Anton, Arpagaus, Belleteix, & Vandamme, 2010; Ma, Jian, Chang, & Yu, 2008; Pathania & Sharma, 2012; Santander-Ortega et al., 2010; Singh, Dartois, et al., 2010; Singh, Singh, et al., 2010). Among these properties, the rheological properties reflect the dispersibility of the starch nanoparticles in aqueous solution which is one of the important aspects concern-

ing their application either solely or as a part of a mixture (Kho & Hadinoto, 2010; Kimura et al., 2011).

Specifically, rheological properties encompass viscous and viscoelastic properties, which all depend on the applied shear rate and the temperature and frequency of the sample. And the creep-recovery is also one of the most important rheological properties of suspensions especially those containing macromolecular compounds. Because of the above mentioned reasons, it is essential to have greater understanding of rheological properties of suspension containing the novel starch nanoparticles. Meanwhile, it has been suggested that electrostatic forces play important role in the dispersion process of nanoparticles into water and other electrolyte solution because the polymeric nanoparticles carry surface charge. And the ionic additives (such as sodium chloride, NaCl) conveniently interact and influence the surface charge, which also can affect the dispersion of starch nanoparticles. Hence, it is expected that rheological properties of suspension containing starch nanoparticles will be affected by the presence or inclusion of salts (Gustafsson, Mikkola, Jokinen, & Rosenholm, 2000; Li, Hou, & Shen, 2009; Köksoy & Kılıç, 2003).

Recently a number of papers have been published reporting the effect of ionic strength of salts on the rheological properties of suspension or gel (Sosa-Herrera, Lozano, Ponce de León, & Martínez-Padilla, 2012; Wittmar, Ruiz-Abad, & Ulbricht, 2012). These studies have shown that salts (including NaCl) affect the viscosity, storage and loss modulus, and gelatination properties quite significantly. A number of researchers have investigated the

\* Corresponding author. Tel.: +86 10 62737351; fax: +86 10 62737351.

E-mail address: [wlj@cau.edu.cn](mailto:wlj@cau.edu.cn) (L.-j. Wang).

<sup>1</sup> These authors contributed equally to this work.

## Nomenclature

$c$	consistency (s)
$E_K$	modulus of the Kelvin spring (Pa)
$E_M$	modulus of the Maxwell spring (Pa)
$G'$	storage modulus (Pa)
$G''$	loss modulus (Pa)
$K$	consistency index ( $\text{Pa s}^n$ )
$K'$	index ( $\text{Pa s}^n$ )
$K''$	index ( $\text{Pa s}^n$ )
$m$	flow behavior index (dimensionless)
$n'$	frequency exponent (dimensionless)
$n''$	frequency exponent (dimensionless)
$R^2$	correlation coefficient (dimensionless)
$T$	absolute temperature (K)
$\tau$	retardation time (s)
$\tau_2$	relaxation time (s)
$t$	loading time (s)
$\eta_M$	viscosity of the Maxwell dashpot ( $\text{Pa s}$ )
$\eta_K$	viscosity of the Maxwell spring dashpot ( $\text{Pa s}$ )
$\omega$	angle frequency (rad/s)
$\delta$	loss angle ( $^\circ$ )
$\dot{\gamma}$	shear rate ( $\text{s}^{-1}$ )
$\eta$	apparent viscosity ( $\text{Pa s}$ )
$\eta_0$	viscosity at zero shear rate ( $\text{Pa s}$ )
$\eta_\infty$	viscosity at infinite shear rate ( $\text{Pa s}$ )
$\varepsilon$	strain of suspension (dimensionless)
$\sigma_0$	constantly applied compressive stress (Pa)

effect of addition of salt on the rheological properties of suspension containing non-starch nano or microparticles. Amiri et al. (2009) investigated the effect of salt concentration on the viscoelastic characteristics of silica suspension and found that an increase in salt concentration increased both storage and loss moduli in the frequency range studied (0.01–10 Hz). Nasser and James (2009) also studied the effect of electrolyte concentration on the rheological behavior of kaolinite suspensions containing microparticles. These authors found that the particle-to-particle interactions between the kaolinite particles and the interaction between the electrolyte charge and kaolinite particles affected the viscoelastic parameters and extent of thixotropy in the suspension. And there are also some researches on the interaction between ionic and counter-ionic components, which could explain the low molecular weight external electrolyte on the rheological behavior of suspension or gel. Chiotelli, Pilosio, and Le Meste (2002) mentioned that the mechanism of starch gelatinization, which was one kind of rheological behavior, in salt solutions could be attributed to the effect of solute on water properties and direct polymer–solute interactions.

In our recent study we reported that different drying methods used in the process of producing starch nanoparticles affect their rehydration characteristics. We also reported that spray drying and vacuum drying are two most effective drying methods in terms of better yield and desired rehydration characteristics (Shi, Wang, Li, & Adhikari, 2012). However, the effect of the presence of ionic additives in the starch nanoparticle matrix (NaCl in this case) on the drying process as well as on the rehydration and rheological properties of resultant starch nanoparticles suspension was not investigated.

In this context, the aim of this study was to investigate the effect of addition of NaCl (in varying concentration) on the rheological properties of suspensions containing spray dried starch nanoparticles. In addition, the modeling of continuous shear viscosity data were carried out using the Cross model. The modeling of the frequency dependence of elastic and loss moduli data were carried

out using Power law model. Similarly, the creep recoveries versus time data of the suspensions were modeled using Burger's model.

## 2. Materials and methods

### 2.1. Materials

Soluble starch (BR, biological reagent) was produced from potato starch through acid-treating technique and purchased from Beijing Aoboxing Biological Technique Company (Beijing, China). Sodium chloride (AR, analysis reagent), sodium hydroxide (AR), cyclohexane (AR), acetone (AR) and acetic acid (AR) were purchased from Beijing Chemical Company (Beijing, China). Polysorbate 80 (Tween-80, FP, food pure) and sorbitan monooleate (Span-80, FP) were purchased from Tianjing Fuchen Chemical Company (Tianjing, China). Sodium trimetaphosphate (STMP) (AR) was obtained from Tianjing Dengfeng Chemical Company (Tianjing, China). All of these reagents were used without further purification. Deionized water was used throughout the work.

### 2.2. Preparation of starch nanoparticles

The method used to prepare starch nanoparticles is based on the emulsion cross-linking technology that uses a high pressure homogenizer and is reported in our pervious paper (Shi, Li, Wang, Li, & Adhikari, 2011). Briefly, starch (8 g) was firstly dissolved into 30 g NaOH (5%) solution and 2 g sodium trimetaphosphate (STMP) was added into 20 g NaCl (7.5%) solution. These two solutions were quickly mixed and were immediately poured into 150 ml cyclohexane containing emulsifiers (1.44 g Tween-80 and 7.56 g Span-80) to produce w/o emulsion using high speed apparatus (IKA® T25 digital, Staufen, Germany) (10,000 rpm for 2 min). Then the nanoemulsion was prepared using high pressure homogenizer at 10 MPa for 2 cycles. Finally, the starch nanoparticles were obtained after 12 h cross-linking and solidification process (25 °C, with magnetic stirring at 250 rpm). And the optic image of starch nanoparticles in w/o emulsion was presented in Fig. 1(A).

After demulsification with 10% glacial acetic acid and twice washing with acetone, starch nanoparticles from 40 ml mini-emulsion were dissolved into 100 ml deionized water for further drying.

### 2.3. Spray drying of starch nanoparticles

A bench-top spray dryer (GPW120-II, Shandong Tianli Drying Equipment Co., Ltd., Shandong, China) (0.7 mm nozzle orifice diameter, 500 ml/h evaporation capacity, 10 l/min compressed air flow rate, 608 kPa compressed air pressure) was used throughout the spray drying trials. The feed flow rate and inlet temperature were set at 5.4 ml/min and 100 °C, respectively. The powders were collected at the cyclone and finally transferred to zip-lock bags. These spray dried powders were stored in desiccators under desired storage temperature and humidity (25 °C and 10% RH) and the scanning electron microscope photographs was shown in Fig. 1(B).

### 2.4. Preparation of suspension

Five 6% (w/v) starch nanoparticle suspensions containing as 0% salt (0 g NaCl and 0.6 g starch nanoparticles in 10 ml DI water), 5% salt (0.5 g NaCl + 0.6 g starch nanoparticles in 10 ml DI water), 10% salt (1 g NaCl + 0.6 g starch nanoparticles in 10 ml DI water), 15% salt (1.5 g NaCl + 0.6 g starch nanoparticles in 10 ml DI water), 20% salt (2 g NaCl + 0.6 g starch nanoparticles in 10 ml DI water) were prepared using a magnetic stirrer for 30 min at 25 °C for rheological tests.

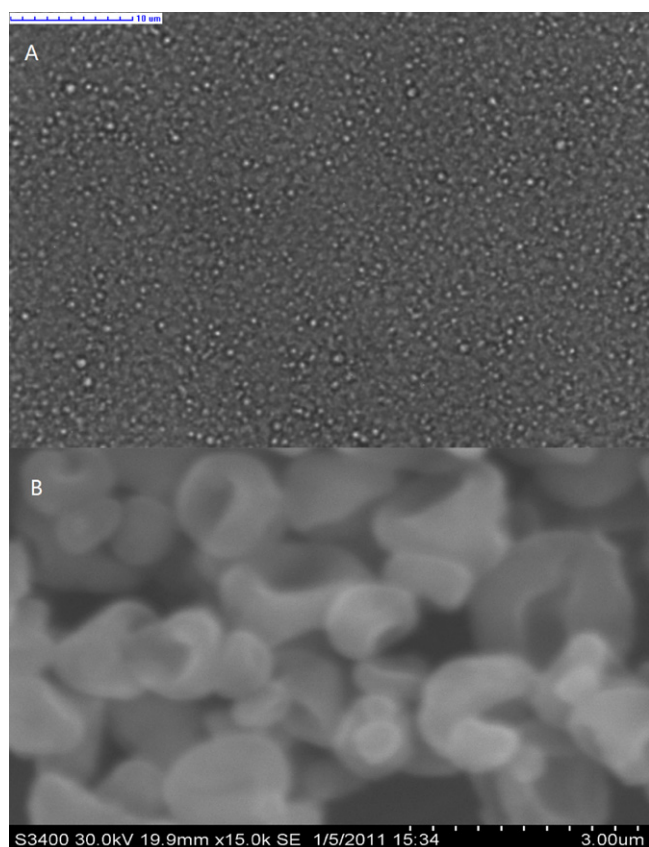


**Fig. 1.** The micro-morphology of starch nanoparticles. (A) Represents starch nanoparticles in w/o emulsion and (B) represents spray dried starch nanoparticles.

## 2.5. Rheological tests

AR2000ex rheometer (TA Instruments Ltd., New Castle, DE) was used for measuring the rheological properties of the suspensions listed Section 2.4. The temperature of the test sample was controlled using a Peltier system at the bottom of the test plate, which was connected to a water bath. A thin layer of silicone oil was applied (during heating cycle) on the surface of the sample in order to prevent evaporation. The linear viscoelastic region was determined for each sample through strain sweeps at 1 Hz (data not shown). Storage modulus ( $G'$ ), loss modulus ( $G''$ ), and loss angle ( $\delta$ ) of the suspensions were determined within the linear viscoelastic region. An equilibration time of 2 min was maintained before each measurement.

### 2.5.1. Continuous shear measurements

The continuous shear tests were performed at 25 °C over the shear rate range of 0.1–100 s<sup>-1</sup> to measure the apparent viscosity. A parallel plate (aluminum, 40 mm diameter, 1 mm gap) was chosen for the continuous shear viscosity measurements.

Specifically, amount of suspension (0.5 ml) described in Section 2.4 was added on the test Peltier board and then the parallel plate dropped to the fixed height to form 1 mm gap. After remove the extra suspension and wipe silica oil on the edge of the plate, the continuous shear measurements were carried out according to above parameters and the data of viscosity were gathered at the same time.

### 2.5.2. Temperature sweep measurements

The temperature sweep measurements were carried out using frequency of 1 Hz and oscillating stress of 0.7958 Pa. The test temperature was increased from 25 °C to 90 °C at a heating rate of

2 °C/min and then decreased to 25 °C at the cooling rate of 2 °C/min. A parallel plate (aluminum, 40 mm diameter, 1 mm gap) was chosen for the temperature ramp measurements.

Specifically, amount of suspension (0.5 ml) described in Section 2.4 was added on the test Peltier board and then the parallel plate dropped to the fixed height to form 1 mm gap. After remove the extra suspension and wipe silica oil on the edge of the plate, the temperature sweep measurements were carried out according to above parameters and the data of modulus were gathered at the same time.

### 2.5.3. Frequency sweep measurements

The frequency sweep tests were performed at 25 °C over the angular frequency range of 0.1–10 rad/s. The oscillating stress for the frequency sweep measurements was selected as 0.7958 Pa based on the strain sweep results (data not shown) in order to confine within the linear viscoelastic region of all the samples. A parallel plate (aluminum, 40 mm diameter, 1 mm gap) was chosen for these frequency sweep measurements.

Specifically, amount of suspension (0.5 ml) described in Section 2.4 was added on the test Peltier board and then the parallel plate dropped to the fixed height to form 1 mm gap. After remove the extra suspension and wipe silica oil on the edge of the plate, the frequency sweep measurements were carried out according to above parameters and the data of modulus were gathered at the same time.

### 2.5.4. Creep-recovery measurements

Creep-recovery experiments were carried out using a shear stress of 7.958 mPa at 25 °C. The variation in shear strain in response to the applied shear stress was measured over a period of 5 min. The shear stress was subsequently removed, and the changes in strain were recorded for a further period of 5 min. A parallel plate (aluminum, 40 mm diameter, 1 mm gap) was chosen for these creep-recovery measurements.

Specifically, amount of suspension (0.5 ml) described in Section 2.4 was added on the test Peltier board and then the parallel plate dropped to the fixed height to form 1 mm gap. After remove the extra suspension and wipe silica oil on the edge of the plate, the creep-recovery measurements were carried out according to above parameters and the data of strain were gathered at the same time.

## 2.6. Statistical analysis

All of these rheological measurements were carried out in triplicate. The experimental rheological data were obtained directly from the TA Rheology Advantage Data Analysis software V 5.4.7 (TA Instruments Ltd., New Castle, DE). The average of three experimental runs was reported as the measured value with standard deviation.

Duncan's multiple comparison method was used to determine the significant effect of presence of NaCl on the rheological properties of the suspensions containing spray dried starch nanoparticles. A confidence level was set at  $p < 0.05$  and the SAS software (SAS Institute Inc., Cary, NC, USA) was used in these statistical analyses. The apparent viscosity data were modeled according to Cross model which is frequently used for suspensions, dispersions, polymer solutions or melts. The frequency sweep results were modeled using Power law model, and the creep data were modeled using to Burger's model, using an inbuilt non-linear regression feature in SPSS 13.0 (SPSS Inc., Chicago, USA).



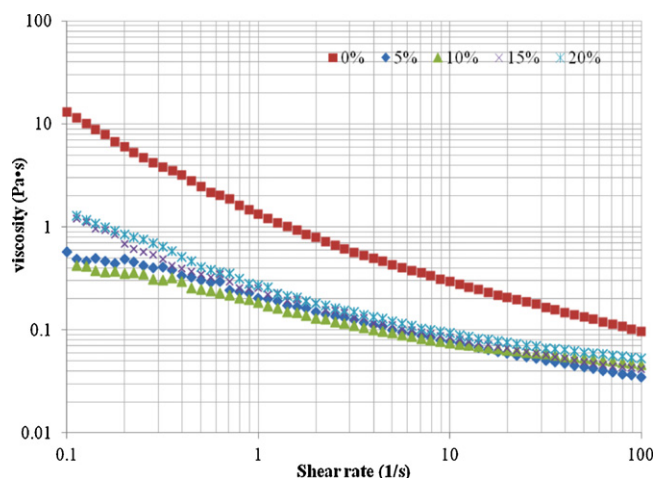


Fig. 2. Effect of the NaCl concentration (w/w) on the apparent viscosity of 6% (w/v) spray dried starch nanoparticles suspension.

### 3. Results and discussion

#### 3.1. The preparation of dried starch nanoparticles

Fig. 1 shows the micro-morphology of starch nanoparticles and according to our previous research (Shi et al., 2011), the starch nanoparticles was cross-linked in the w/o micro-emulsion and displayed a size of 300–500 nm (Fig. 1(A)). And in Fig. 1(B) the SEM photograph of spray dried starch nanoparticles shows a size around 1000 nm. It was quite larger than that in w/o emulsion and the possible reason might be result from the nozzle of spray dryer was the main factor to decide the size of droplets and these droplets might contain lot of starch nanoparticles. And the dried starch particle was possible to be composed of several starch nanoparticles. And the swelling of starch nanoparticles, which would enlarge the size of starch nanoparticle in water, also could be the possible reason.

#### 3.2. Continuous shear measurements

Fig. 2 presents the steady state flow curves of 6% (w/v) suspension of spray dried starch nanoparticles with varying NaCl concentration. It can be seen from this figure that the addition of NaCl results into the decrease in the apparent viscosity of suspension within the entire shear rate ( $0.1\text{--}100\text{ s}^{-1}$ ) tested. This figure also shows that these starch nanoparticle suspensions with or without the presence of NaCl exhibit shear-thinning behavior within the entire shear rate range ( $0.1\text{--}100\text{ s}^{-1}$ ). The shear thinning behavior of these suspensions (in the presence or absence of NaCl) can be attributed to the fact that the aggregated particles begin to separate as the shear rate increases and the suspensions become increasingly uniform. The apparent viscosity data shown in this figure also suggest that the increase in the NaCl concentration from 5% to 20% does not alter the shear thinning trend. The increase in the NaCl concentration only alters the magnitude of the consistency coefficients and flow behavior indices. The interesting feature regarding the effect of addition of NaCl at different concentration (Fig. 2) is that the viscosity of the suspension decreases very rapidly at low shear rates ( $0.1\text{--}10\text{ s}^{-1}$ ) when the concentration of NaCl is increased from 0% to 10% because of the shielding or screening action of sodium counterions. At the same shear rates ( $0.1\text{--}10\text{ s}^{-1}$ ), concentrations above 10%, i.e. 15% and 20%, lead to increases in viscosity, attributable to solvation of Na ions “forcing” nanoparticles to associate themselves. When the shear rate is above  $10\text{ s}^{-1}$ , the viscosity of starch nanoparticles suspension in the presence of NaCl increases only marginally when the concentration of NaCl is higher.

At low shear rates where the effect of mechanical shearing is not strong, the significant ( $p < 0.05$ ) decrease in viscosity (compared to the viscosity of starch nanoparticles only (0% salt) suspensions) at 5–10% NaCl concentration can be attributed to the compression of electric double layer (EDL) and consequential reduction in repulsion between the starch nanoparticles at low NaCl concentration (Saleh et al., 2008). However, when an excess amount of NaCl is added ( $>10\%$  in this case), it induces coagulation which could explain the slight increase in the viscosity (Xin, Xu, Wu, Li, & Cao, 2007) due to increase in the NaCl concentration. The shear stress versus shear rate data of the aqueous NaCl solutions within the concentration range (at  $20^\circ\text{C}$ ) are known to vary linearly and the Newtonian viscosity values of the solutions have reported to be varying from  $1.076 \times 10^{-3}\text{ Pa s}$  (at 5%) to  $1.418 \times 10^{-3}\text{ Pa s}$  (at 20%) (Kestin, Khalifa, & Correia, 1981). This means that even the lowest viscosity value of the starch nanoparticle suspensions is 100 times higher than the viscosity values of the salt solutions. These low viscosity values of the salt solutions suggests that the effect of the salt is not due to bulk mixing rule in viscosity rather it is the effect of ions on electric double layer.

As shown in Fig. 2, the viscosity of the starch nanoparticle suspension was the lowest at high shear rates when the concentration of the NaCl was 5%. High concentration of NaCl might decrease the Debye's length of starch nanoparticles and expose their molecular structure because of the compression of electric double layer (EDL). Therefore, the violent collisions (induced by shearing) between nanoparticles in suspension could induce coagulation which was more apparent at higher NaCl concentrations. Another possible reason for the effect of NaCl on the viscosity of suspension might concern the water activity, osmotic pressure and boiling point of suspension. When the concentration of NaCl was high (15% and 20%), that the water activity was low and the osmotic pressure and boiling point was high might affect the interactions among starch nanoparticles.

We also modeled the flow curves or experimental viscosity versus shear rate data (Susan-Resiga, Bica, & Vékás, 2010) using Cross model (Eq. (1)), which is commonly used model representing the trend and characteristics of suspensions during continuous shear.

$$\eta = \eta_{\infty} + \frac{\eta_0 - \eta_{\infty}}{1 + (C\dot{\gamma})^m} \quad (1)$$

Here  $\eta$  is the apparent viscosity (Pa s),  $\eta_{\infty}$  is the viscosity at infinite shear rate (Pa s),  $\eta_0$  is the viscosity at zero shear rate (Pa s),  $c$  is the consistency (s),  $\dot{\gamma}$  is the shear rate ( $\text{s}^{-1}$ ), and  $m$  is the flow behavior index (dimensionless) (Corcione, Cavallo, Pesce, Greco, & Maffezzoli, 2011).

The parameters obtained by fitting the Cross model to experimental data are presented in Table 1. This table shows that the viscosity values both at zero and infinite shear rates are significantly ( $p < 0.05$ ) reduced by adding NaCl. As can be seen from this table, the viscosity values at zero shear rate at different NaCl concentrations firstly decreased from 35.015 Pa s to 0.438 Pa s when the NaCl concentration increased from 0% to 10%. Subsequently, when the NaCl concentration increased from 10% to 20%, the viscosity increased (instead of decreasing continuously) from 0.438 Pa s to 2.507 Pa s. However, the viscosity values at infinite shear rate are not statistically different and there is no clear increasing or decreasing trend when the NaCl concentration is over 5%. The  $c$  and  $m$  values of suspensions (Table 1) indicate that the presence of NaCl can weaken the shear thinning behavior and to some extent, make the suspension more stable during the shearing process.

**Table 1**Cross modeling parameters of apparent viscosity of 6% (w/v) suspension of spray dried starch nanoparticles containing different NaCl concentration (w/v).<sup>a</sup>

NaCl concentration (% w/v)	$\eta_0$ (Pa s)	$\eta_\infty$ (Pa s)	$c$ (s)	$m$ (dimensionless)	$R^2$
0	35.015 ± 6.115 <sup>a</sup>	0.279 ± 0.029 <sup>a</sup>	20.923 ± 4.210 <sup>a</sup>	0.895 ± 0.038 <sup>a</sup>	0.998
5	0.557 ± 0.012 <sup>b</sup>	0.030 ± 0.006 <sup>b</sup>	4.947 ± 0.521 <sup>b</sup>	0.641 ± 0.042 <sup>b</sup>	0.993
10	0.438 ± 0.007 <sup>b</sup>	0.042 ± 0.003 <sup>c</sup>	4.896 ± 0.370 <sup>b</sup>	0.644 ± 0.029 <sup>b</sup>	0.997
15	1.479 ± 0.120 <sup>c</sup>	0.096 ± 0.009 <sup>d</sup>	5.412 ± 1.153 <sup>b</sup>	0.701 ± 0.029 <sup>c</sup>	0.969
20	2.507 ± 0.266 <sup>d</sup>	0.055 ± 0.003 <sup>e</sup>	19.063 ± 3.270 <sup>a,c</sup>	0.819 ± 0.018 <sup>d</sup>	0.999

<sup>a</sup> Values represent the mean ± standard deviation of triplicate tests. Values in a column with different superscripts were significantly different ( $p < 0.05$ ).

### 3.3. Temperature sweep measurements

Fig. 3 displays the variation in storage modulus ( $G'$ ), loss modulus ( $G''$ ), and loss angle ( $\delta$ ) as a function of temperature. The temperature of the suspension was first increased from 25 °C to 90 °C, and then decreased to 25 °C. As can be seen from Fig. 3(A), the storage modulus of starch nanoparticles suspension in the absence of NaCl and in the presence of NaCl shows same trends with the change in temperature. And the suspension in the absence of NaCl has a higher value of  $G'$  than other suspension containing NaCl. This might be due to the fact that NaCl could affect the electric double layers of starch nanoparticles, and change the density, and then finally influence the elasticity and collision in suspension, which could result in the increase in the storage modulus.

From Fig. 3(B) it can be seen that the trend of variation in the loss modulus ( $G''$ ) of all these NaCl containing suspensions at all the NaCl concentration levels is similar within the entire temperature range. Specifically, when the temperature of suspensions increases (from 25 °C to 90 °C), the loss modulus decreases first before increasing. During the cooling process (90–25 °C), the loss modulus recovers to the value which is slightly higher than the initial value. Fig. 3(B) also shows that the effect of varying NaCl concentration on loss modulus is similar to its effect on viscosity as presented and explained in Section 3.1. The loss modulus decreases first when the NaCl concentration increases from 0% to 15%, subsequently it increases with the increase in the NaCl concentration (15–20%). When small amount of NaCl is added into the suspension containing starch nanoparticles, the presence of NaCl causes the compression of electric double layer (EDL). As a consequence, when the concentration of NaCl increases, the viscosity which can be calculate from loss modulus (Barnes, Hutton, & Walter, 1989) decreases because of the weakening of interaction among starch nanoparticles. And, when large or excess amount of NaCl was present in the suspension, it induced coagulation which explained the increase in loss modulus (viscosity) (Xin et al., 2007).

The value of loss angle ( $\delta$ ) is commonly used to explain the gelling properties of suspension containing macromolecules. From Fig. 3(C), all suspensions shows remarkable drop in loss angle which is resulted from the gelling of starch nanoparticles. These results suggest that the presence of NaCl affects internal structure of suspension during heating and cooling and finally affects the storage modulus, loss modulus and loss angle.

### 3.4. Frequency sweep measurements

Fig. 4 shows the frequency dependence for storage modulus ( $G'$ ), loss modulus ( $G''$ ) and loss angle ( $\delta$ ) of suspensions containing 6% (w/v) starch nanoparticles and different amount of NaCl (0–20%, w/w). As can be seen from this figure, loss modulus ( $G''$ ) values of all the suspensions are higher than the corresponding values of storage modulus ( $G'$ ) over the entire frequency range studied (0.1–10 rad/s). This observation suggests that suspensions of the starch nanoparticles exhibit dominant viscous behavior (than elastic behavior), no matter how much NaCl is added (within 20% NaCl concentration studied). In all these suspensions, the storage and loss modulus increased and loss angle decreased when the angular frequency increased. This might have been resulted from the alteration in the internal structure of suspension under oscillating stress (Li & Huang, 2012). It can also be observed from Fig. 4 that the addition (presence) of NaCl can affect the storage modulus, loss modulus and loss angle quite significantly ( $p < 0.05$ ). However, the increase in the NaCl concentration above 5% concentration does not have significant ( $p > 0.05$ ) effect on these values. The reduction in the storage and loss modulus can also be explained based on the fact that the presence of NaCl affects the internal structure of the suspension which has been observed in continues shear and temperature sweep measurements. At higher oscillating frequencies, the starch nanoparticles have higher probability of colliding among themselves during the oscillation process. The increase in

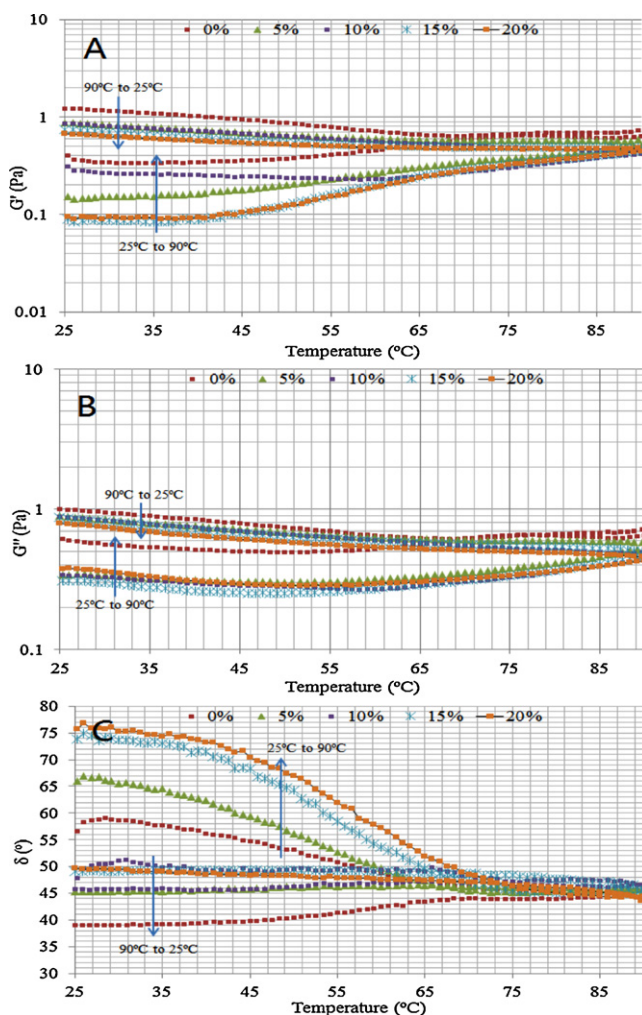


**Fig. 3.** The variation of viscoelastic modulus with temperature of 6% (w/v) spray dried starch nanoparticles suspension containing different NaCl concentration (w/w).

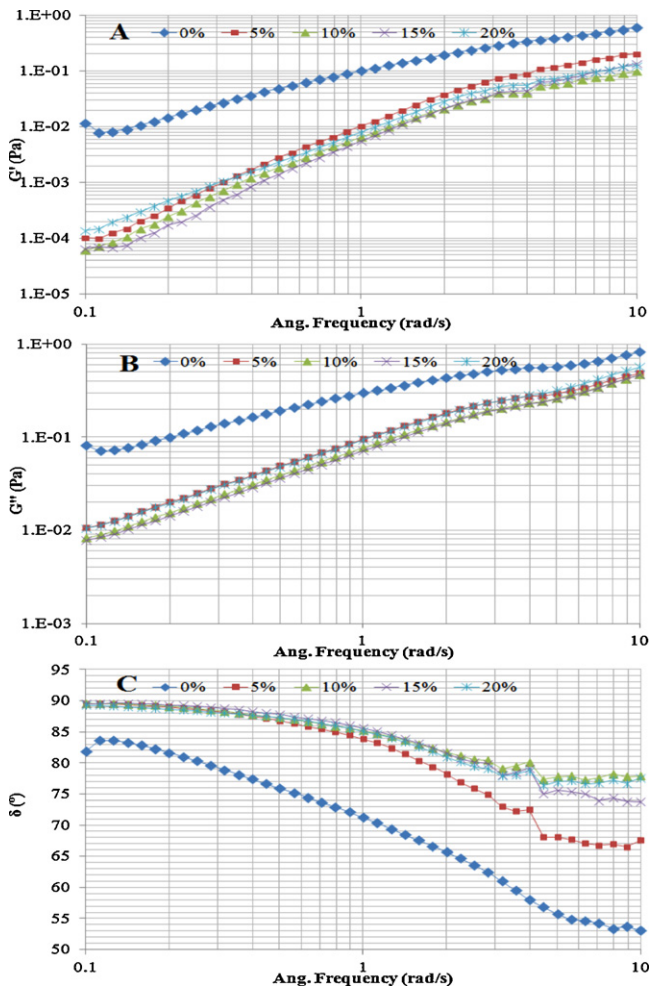


**Fig. 4.** Frequency dependence of 6% (w/v) spray dried starch nanoparticles suspension containing different NaCl concentration (w/w).

the kinetic (due to higher mechanical energy input) energy finally gets transformed into the increase in the storage and loss modulus. This is the reason why the increase in the NaCl concentration (above 5%) did not alter the trend and magnitude of the storage and loss modulus of these suspensions. On the other hand, the loss angle showed decreasing trend when the angular frequency increased within the frequency range studied (Fig. 4(C)). This observation suggests that the rate of increase in the loss modulus is higher than the rate of increase in the loss modulus when oscillating frequency is increased. This is the reason why the elastic behavior of the suspension was more dominant. The presence of NaCl can reduce both the storage modulus and loss modulus of the suspensions. However, the presence of NaCl brings in higher reduction in the storage modulus than the loss modulus. This is the reason why the loss angle showed remarkable increase in Fig. 4(C) when NaCl was added into the suspension. The loss angle decreased with the increase in the oscillation frequency. The trend in the variation of loss angle with frequency is similar both in the presence and absence of NaCl (Fig. 4(C)).

We used Power law models, represented by Eqs. (2) and (3) to analyze the frequency dependence of  $G'$  and  $G''$  (Wang, Wang, Li, Xue, & Mao, 2009).

$$G' = K' \cdot \omega^{n'} \quad (2)$$

$$G'' = K'' \cdot \omega^{n''} \quad (3)$$

where  $K'$  and  $K''$  are Power law constants and reflect the elastic and viscous properties, respectively.  $n'$  and  $n''$  are referred to as the frequency exponents and  $\omega$  is the angular frequency (rad/s).

The Power law parameters of  $G'$  and  $G''$  for these suspensions are presented in Table 2. As can be seen from this table, the regression coefficients are higher than 0.98 and the average absolute error ranged from 0.30% to 2.70% which suggests that the Power law model represents the experimental  $G'$  and  $G''$  data well. The  $K''$  values of all these suspensions are slightly higher than the  $K'$  values (at the same angular frequency), indicating that the suspensions containing starch nanoparticles display higher viscous effect than elastic effect within the frequency range of 0.1–10 rad/s. This observation corroborates well with the fact that the loss angles of all the suspension were always very high (53–89°). Furthermore, the suspensions containing NaCl have lower  $K'$  and  $K''$  values compared to the suspensions without NaCl which is also in accord with the results presented in Fig. 4. The suspensions containing only starch nanoparticles were always more elastic than viscous compared to the suspensions containing NaCl. It can also be seen from Table 2 that both the elastic and viscous components of suspensions containing NaCl reached their corresponding lowest values when the NaCl concentration was 15%. This observation suggests that the addition of small concentration of NaCl can lower both the elastic and viscous components of suspension (containing starch nanoparticles) while the presence of higher concentration of NaCl can produce the opposite results. The  $n'$  and  $n''$  values of suspension containing only starch nanoparticles are slightly lower than the suspensions containing NaCl. This observation indicates that the presence of NaCl enhances the frequency sensitivity of starch nanoparticles suspensions (Wang et al., 2009). However, the increase in NaCl concentration from 5% to 20% did not exhibit much effect on the  $n'$  and  $n''$  values.

### 3.5. Creep-recovery measurements

The creep-recovery behavior of starch nanoparticles suspensions in the absence and presence (in varying concentration) of NaCl is shown in Fig. 5(A). The strain versus time data presented in this figure show that the suspension in the absence of NaCl deformed the most during the creep test, while suspension containing 20% (w/w) NaCl deformed the least, among all the samples.

Burger's model (Eq. (4)), which is comprised of both the Maxwell and Kelvin models arranged in series (Jia, Peng, Gong, & Zhang, 2011), is used to describe the creep recovery behavior.

$$\varepsilon = \frac{\sigma_0}{E_M} + \frac{\sigma_0}{E_K}(1 - e^{-t/\tau}) + \frac{\sigma_0}{\eta_M} \cdot t \quad (4)$$

$$\tau = \frac{\eta_K}{E_K} \quad (5)$$

where  $\varepsilon$  represents the strain (%) of suspension,  $t$  represents the time (s) after loading,  $E_M$  and  $\eta_M$  are the modulus (Pa) and viscosity (Pa s) of the Maxwell spring and dashpot, respectively. Similarly,  $E_K$  and  $\eta_K$  are the modulus (Pa) and viscosity (Pa s) of the Kelvin spring and dashpot, respectively. Similarly,  $\tau = \eta_K/E_K$  is the time taken to recover 63.2% or  $(1 - e^{-1})$  of the total deformation in the Kelvin unit. The parameters  $E_M$ ,  $E_K$ ,  $\eta_M$ , and  $\tau$  were obtained from fitting the experimental data to Eqs. (4) and (5) with SPSS software.

Fig. 5(B) and (C) are the enlarged or zoomed view of the first 5 s of the creep section and the recovery section, respectively. And, it can be seen from Fig. 5 (B) that there is no instantaneous strain within the first 1 s (Wang et al., 2009). The modulus of Maxwell spring ( $E_M$ ) which is calculated using the height of the linear section of the curve is not seen in Fig. 5(B). In Maxwell unit, the instantaneous elastic deformation of spring does not exist. Hence, the main effect of Maxwell unit can be attributed to the viscous flow deformation of dashpot. Furthermore, the entire curve consists of recovered elastic



**Table 2**Power law modeling parameters of elastic modulus of 6% (w/v) spray dried starch nanoparticles suspension contain different NaCl concentration (w/v).<sup>a</sup>

NaCl concentration (% w/v)	$K'$ (Pa s <sup>n</sup> )	$n'$ (dimensionless)	$R^2$	$K''$ (Pa s <sup>n</sup> )	$n''$ (dimensionless)	$R^2$
0	0.109 ± 0.003 <sup>a</sup>	0.762 ± 0.017 <sup>a</sup>	0.991	0.282 ± 0.006 <sup>a</sup>	0.461 ± 0.013 <sup>a</sup>	0.981
5	0.020 ± 0.001 <sup>b</sup>	1.054 ± 0.033 <sup>b</sup>	0.986	0.100 ± 0.003 <sup>b</sup>	0.690 ± 0.016 <sup>b</sup>	0.989
10	0.011 ± 0.001 <sup>c</sup>	0.998 ± 0.029 <sup>c</sup>	0.987	0.079 ± 0.002 <sup>c</sup>	0.762 ± 0.012 <sup>c</sup>	0.995
15	0.009 ± 0.001 <sup>c</sup>	1.175 ± 0.024 <sup>d</sup>	0.994	0.075 ± 0.002 <sup>c</sup>	0.788 ± 0.013 <sup>d</sup>	0.995
20	0.014 ± 0.001 <sup>d</sup>	0.984 ± 0.031 <sup>e</sup>	0.985	0.095 ± 0.002 <sup>d</sup>	0.767 ± 0.011 <sup>e</sup>	0.996

<sup>a</sup> Values represent the mean ± standard deviation of triplicate tests. Values in a column with different superscripts were significantly different ( $p < 0.05$ ).**Table 3**Burger's modeling parameters of creep-recovery behavior of 6% (w/v) spray dried starch nanoparticles suspension contain different NaCl concentration (w/v).<sup>a</sup>

NaCl concentration (% w/v)	$E_2$ (Pa)	$\tau_2$ (s)	$\eta_1$ (Pa s)	$R^2$	Recovery (%)
0	0.173 ± 0.002 <sup>a</sup>	2.286 ± 0.085 <sup>a</sup>	26.768 ± 0.349 <sup>a</sup>	0.982	57.7
5	0.210 ± 0.002 <sup>b</sup>	1.395 ± 0.054 <sup>b</sup>	58.391 ± 1.338 <sup>b</sup>	0.969	56.8
10	0.285 ± 0.004 <sup>c</sup>	0.804 ± 0.037 <sup>c</sup>	174.080 ± 10.563 <sup>c</sup>	0.914	84.1
15	0.692 ± 0.014 <sup>d</sup>	0.578 ± 0.023 <sup>d</sup>	246.160 ± 8.140 <sup>d</sup>	0.937	86.5
20	1.229 ± 0.021 <sup>e</sup>	0.368 ± 0.017 <sup>e</sup>	203.783 ± 3.789 <sup>e</sup>	0.944	30.6

<sup>a</sup> Values represent the mean ± standard deviation of triplicate tests. Values in a column with different superscripts were significantly different ( $p < 0.05$ ).

deformation ( $E_K$ ) of Kelvin spring and viscous flow deformation ( $\eta_M$ ) of Maxwell dashpot. The viscous flow deformation of Kelvin dashpot also exerts some degree of effect on the recovery time. And, the recovery section shown in Fig. 5(C), also illustrates these results.

Parameters for the Burger's model for all the tested suspensions are listed in Table 3. The Burger's model fitted the experimental strain versus time data reasonably well ( $R^2 > 0.91$ , average absolute errors 0.08–2.73%). The fitting of the model returns the  $E_M$  value to be zero as explained in the preceding paragraph and is not shown in the table. Among all these suspensions, the suspension containing only starch nanoparticles shows the lowest  $E_K$  and  $\eta_M$  values and the highest  $\tau$  value. At the same time, the suspension containing 20% (w/w) NaCl displays the highest  $E_K$  value and the lowest  $\tau$  value. The suspension containing 15% (w/w) NaCl has highest  $\eta_M$  value of 246 Pa s even higher than  $\eta_M$  value (204 Pa s) of the suspension containing 20% (w/w) NaCl.

Here, the  $E_K$  value shows the recovered elastic deformation of suspension under steady and uniform pressure and  $\eta_M$  value is a reflection of the viscosity of the samples. In Table 2, the lowest  $K'$  and  $K''$  value mean that the suspension containing 15% NaCl has lower viscous and elastic modulus than other suspensions. Meanwhile, the very high loss angle value shows the dominance of viscous component in these suspensions. Based on the results presented in Tables 2 and 3, it can be stated that the addition of NaCl can lead to larger reduction in viscous component than the elastic component which can affect the recovery rates. Table 3 also shows that the recovery rate is at its highest value when the suspension contained 15% (w/w) NaCl (Ruiz Martinez et al., 2007). However, high concentration of NaCl (>15%) has an adverse effect on the creep recovery which is in accordance with the increase of  $K'$  and  $K''$  in Table 2.

#### 4. Conclusion

The effect of NaCl on rheological properties such as viscosity, elastic and loss moduli of suspensions of spray dried starch nanoparticles was studied. The effects of increasing continuous shear rate (on viscosity) and angular frequency and heating and cooling cycle (on elastic and loss moduli) viscosity were also studied. The addition of NaCl <15% (w/w) was found to lower the viscosity of the suspensions quite significantly ( $p < 0.05$ ) compared to that of the control (suspension containing only starch nanoparticles) while an excess of NaCl (>15%, w/w) was found to slightly increase the viscosity of the suspension which was still well below the viscosity of the control. The viscosity versus shear rate data were fitted well ( $R^2 > 0.9$  and average absolute errors 0.38–4.15%) by the Cross model. The presence of NaCl was found to enhance the resistance of suspension to the heat destabilization and finally weakened the gelling behavior. The loss modulus values of all

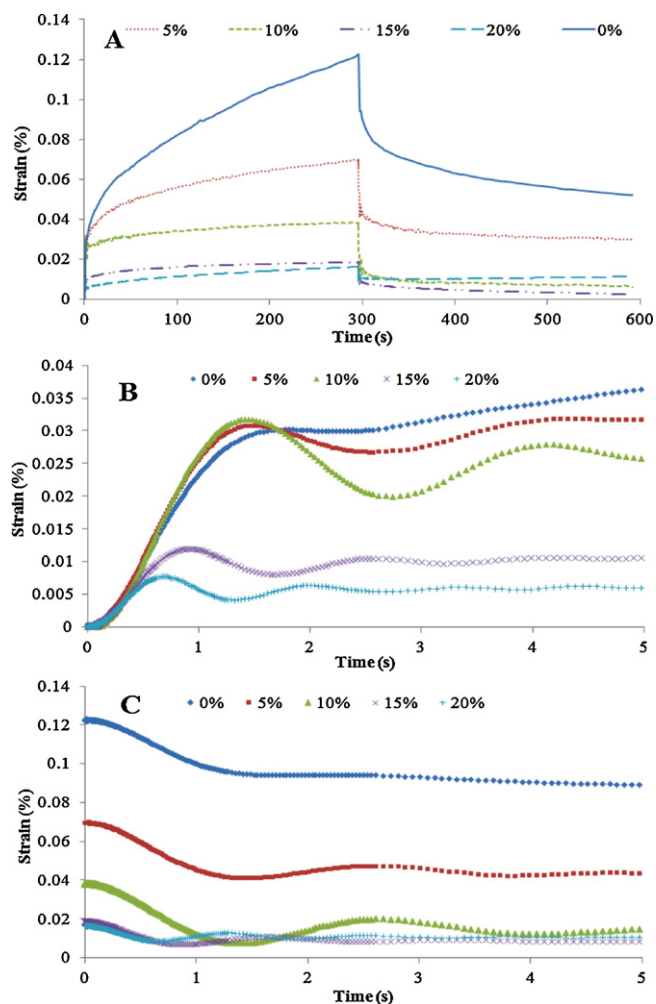


**Fig. 5.** Creep-recovery behaviors of 6% (w/v) spray dried starch nanoparticles suspension containing different NaCl concentration (w/w).

suspensions were higher than storage modulus values the corresponding over the frequency range studied (0.1–10 rad/s). The addition of NaCl was found to affect the storage modulus, loss modulus and loss angle quite considerably. However, increase in salt concentration >5% (w/w) had insignificant ( $p > 0.05$ ) effect on these values. The experimental  $G'$  and  $G''$  data were fitted well by the Power law model ( $R^2 > 0.98$  and average absolute errors 0.30–2.70%). The creep recovery data of the suspensions were fitted using Burger's model and found that the suspension without NaCl had the lowest  $E_K$  (Kelvin elastic modulus) and  $\eta_M$  (Maxwell viscosity) values and highest  $\tau$  (recovery time) value while the suspension containing 20% (w/w) NaCl had the highest  $\eta_K$  (Kelvin modulus) value and the lowest  $\tau$  value. The suspension containing 15% (w/w) NaCl had the highest  $\eta_M$  value even higher than that of the suspension containing 20% (w/w) NaCl. It found that the rate of creep recovery of the suspensions was highest when the concentration of the salt in the suspension was 15% (w/w) and that above this salt concentration the rate of recovery decreased.

## Acknowledgements

This research was supported by National Natural Science Foundation of China (31000813), Chinese Universities Scientific Fund (2012QJ009), High Technology Research and Development Program of China (2011AA100802), and Commonweal Guild Agricultural Scientific Research Project of China (201003077).

## References

- Amiri, A., Øye, G., & Sjöblom, J. (2009). Influence of pH, high salinity and particle concentration on stability and rheological properties of aqueous suspensions of fumed silica. *Colloids and Surfaces A: Physicochemical and Engineering Aspects*, 349, 43–54.
- Barnes, H. A., Hutton, J. F., & Walter, K. (1989). *An introduction to rheology*. Amsterdam: Elsevier., pp 115–137.
- BeMiller, J. N., & Whistler, R. L. (2009). *Starch: Chemistry and technology* (3rd ed.). Academic Press., p. 491.
- Chin, S. F., Pang, S. C., & Tay, S. H. (2011). Size controlled synthesis of starch nanoparticles by a simple nanoprecipitation method. *Carbohydrate Polymers*, 86, 1817–1819.
- Chiotelli, E., Pilosio, G., & Le Meste, M. (2002). Effect of sodium chloride on the gelatinization of starch: A multimeasurement study. *Biopolymers*, 63, 41–58.
- Corcione, C. E., Cavallo, A., Pesce, E., Greco, A., & Maffezzoli, A. (2011). Evaluation of the degree of dispersion of nanofillers by mechanical, rheological, and permeability analysis. *Polymer Engineering and Science*, 51(7), 1280–1285.
- Granö, H., Yli-Kauhaluoma, J., Suortti, T., Käki, J., & Nurmi, K. (2000). Preparation of starch betainate: A novel cationic starch derivative. *Carbohydrate Polymers*, 41(3), 277–283.
- Gustafsson, J., Mikkola, P., Jokinen, M., & Rosenholm, J. B. (2000). The influence of pH and NaCl on the zeta potential and rheology of anatase dispersions. *Colloids and Surfaces A: Physicochemical and Engineering Aspects*, 175, 349–359.
- Jia, Y., Peng, K., Gong, X.-L., & Zhang, Z. (2011). Creep and recovery of polypropylene/carbon nanotube composites. *International Journal of Plasticity*, 27(8), 1239–1251.
- Kestin, J., Khalifa, H. E., & Correia, R. J. (1981). Tables of the dynamic and kinematic viscosity of aqueous NaCl solutions in the temperature range 20–150 °C and the pressure range 0.1–35 MPa. *Journal of Physical and Chemical Reference Data*, 10, 71–88.
- Kho, K., & Hadinoto, K. (2010). Aqueous re-dispersibility characterization of spray-dried hollow spherical silica nano-aggregates. *Powder Technology*, 198, 354–363.
- Kimura, H., Sakurai, M., Sugiyama, T., Tsuchida, A., Okubo, T., & Masuko, T. (2011). Dispersion state and rheology of hectorite particles in water over a broad range of salt and particle concentrations. *Rheologica Acta*, 50, 159–168.
- Köksoy, A., & Kılıç, M. (2003). Effects of water and salt level on rheological properties of ayran, a Turkish yoghurt drink. *International Dairy Journal*, 13, 835–839.
- Le Corre, D., Bras, J., & Dufresne, A. (2010). Starch nanoparticles: A review. *Biomacromolecules*, 11(5), 1139–1153.
- Li, J., & Huang, Q. (2012). Rheological properties of chitosan–tripolyphosphate complexes: From suspensions to microgels. *Carbohydrate Polymers*, 87(2), 1670–1677.
- Li, X., Anton, N., Arpagaus, C., Belleteix, F., & Vandamme, T. F. (2010). Nanoparticles by spray drying using innovative new technology: The Büchi Nano Spray Dryer B-90. *Journal of Controlled Release*, 147, 304–310.
- Li, Y., Hou, W.-G., & Shen, S.-L. (2009). Rheological behavior of aqueous suspensions containing cationic starch and aluminum magnesium hydrotalcite-like compound in the presence of different electrolytes. *Colloids and Surfaces A: Physicochemical and Engineering Aspects*, 350, 109–113.
- Ma, X., Jian, R., Chang, P. R., & Yu, J. (2008). Fabrication and characterization of citric acid-modified starch nanoparticles/plasticized-starch composites. *Biomacromolecules*, 9, 3314–3320.
- Nasser, M. S., & James, A. E. (2009). The effect of electrolyte concentration and pH on the flocculation and rheological behaviour of kaolinite suspensions. *Journal of Engineering Science and Technology*, 4(4), 430–446.
- Pathania, D., & Sharma, R. (2012). Synthesis and characterization of graft copolymers of methacrylic acid onto gelatinized potato starch using chromic acid initiator in presence of air. *Advanced Materials Letters*, 3(2), 136–142.
- Ruiz Martinez, Ma. A., López-Viata Gallardo, J., de Benavides, M. M., de Dios García López-Duran, J., & Gallardo Lara, V. (2007). Rheological behavior of gels and meloxicam release. *International Journal of Pharmaceutics*, 333(1–2), 17–23.
- Saleh, N., Kim, H.-J., Phenrat, T., Matyjaszewski, K., Tilton, R. D., & Lowry, G. V. (2008). Ionic strength and composition affect the mobility of surface-modified FeO nanoparticles in water-saturated sand columns. *Environmental Science & Technology*, 42, 3349–3355.
- Santander-Ortega, M. J., Stauner, T., Loretz, B., Ortega-Vinuesa, J. L., Bastos-González, D., Wenz, G., et al. (2010). Nanoparticles made from novel starch derivatives for transdermal drug delivery. *Journal of Controlled Release*, 141, 85–92.
- Shi, A.-M., Li, D., Wang, L.-J., Li, B.-Z., & Adhikari, B. (2011). Preparation of starch-based nanoparticles through high-pressure homogenization and miniemulsion cross-linking: Influence of various process parameters on particle size and stability. *Carbohydrate Polymers*, 83(4), 1604–1610.
- Shi, A.-M., Wang, L.-J., Li, D., & Adhikari, B. (2012). The effect of annealing and cryoprotectants on the properties of vacuum-freeze dried starch nanoparticles. *Carbohydrate Polymers*, 88, 1334–1341.
- Simi, C. K., & Emilia Abraham, T. (2007). Hydrophobic grafted and cross-linked starch nanoparticles for drug delivery. *Bioprocess Biosystem Engineering*, 30, 173–180.
- Singh, J., Dartois, A., & Kaur, L. (2010). Starch digestibility in food matrix: A review. *Trends in Food Science & Technology*, 21, 168–180.
- Singh, V., Singh, S. K., Pandey, S., & Sanghi, R. (2010). Adsorption behavior of potato starch–silica nanobiocomposite. *Advanced Materials Letters*, 1(1), 40–47.
- Sosa-Herrera, M. G., Lozano, I. E., Ponce de León, Y. R., & Martínez-Padilla, L. P. (2012). Effect of added calcium chloride on the physicochemical and rheological properties of aqueous mixtures of sodium caseinate/sodium alginate and respective oil-in-water emulsions. *Food Hydrocolloids*, 29(1), 175–184.
- Susan-Resiga, D., Bica, D., & Vékás, L. (2010). Flow behaviour of extremely bidisperse magnetizable fluids. *Journal of Magnetism and Magnetic Materials*, 322(20), 3166–3172.
- Wang, Y., Wang, L.-J., Li, D., Xue, J., & Mao, Z.-H. (2009). Effects of drying methods on rheological properties of flaxseed gum. *Carbohydrate Polymers*, 78(2), 213–219.
- Wittmar, A., Ruiz-Abad, D., & Ulbricht, M. (2012). Dispersions of silica nanoparticles in ionic liquids investigated with advanced rheology. *Journal of Nanoparticle Research*, 14, 651.
- Xin, X., Xu, G., Wu, D., Li, Y., & Cao, X. (2007). The effect of CaCl<sub>2</sub> on the interaction between hydrolyzed polyacrylamide and sodium stearate: rheological property study. *Colloids and Surfaces A: Physicochemical and Engineering Aspects*, 305, 138–144.